purposes, the strength coefficient for an overlay be taken as half the strength coefficient of asphalt concrete.

Taking the strength coefficient of an asphalt concrete overlay as half the value for new construction can be justified as follows. As a pavement ages and is trafficked, it becomes fatigued and weak. When an underlying layer becomes weaker than the overlying one, the thickness equivalency of the overlying layer decreases. This is illustrated by the practice in Virginia of taking the thickness equivalency of a cement-treated aggregate placed directly over a raw subgrade as 0.6 times its thickness equivalency when placed over a strong subbase or a base course.

THICKNESS OF AN OVERLAY

By using Equation 2a, the traffic carried by an overlaid pavement can be calculated as

$$\text{Traffic} = \text{antilog}(C_a + 1.1D_a) - \text{antilog}(C_b - 1.1D_b) \quad (4)$$

where C_b and C_a = values of C in Equation 2a before the overlay and at the end of the overlay service period, respectively.

In the AASHO Road Test, the SIs before the overlay and at the end of the service period of the overlay were not the same. In practice, these values are the same, depending on the road classification; i.e., $C_a = C_b$, and Equation 3 reduces to

$$\text{Traffic after overlay} = \text{traffic before overlay} \times \{\text{antilog}[0.11 \times (\text{overlay thickness}/2.5) \times \text{strength coefficient of overlay}] - 1\} \quad (5a)$$

(when overlay thickness is measured in centimeters) or

$$\text{Traffic after overlay/traffic before overlay} = \{\text{antilog}[0.11 \times 0.22 \times (\text{overlay thickness}/2.5)] - 1\} = [\text{antilog}(0.01 \times \text{overlay thickness}) - 1] \quad (5b)$$

or

$$\text{Percentage increase in traffic after overlay} = \text{antilog}(0.01 \times \text{overlay thickness}) - 1 \times 100 \quad (5c)$$

As shown by Vaswani in Figure 4 of the previous paper in this Record, the relationship between the percentage increase in the accumulated traffic and the overlay thickness can be used to determine the required thickness of an overlay. This figure shows that the traffic capacities for overlay thicknesses of 2.5, 5.1, and 7.6 cm (1, 2, and 3 in) are, respectively, 78, 217, and 464 percent of the traffic before the overlay.

If these percentage increases in traffic are examined carefully, it is seen that the percentage increase in traffic would be the same if the overlay were applied in several thin layers rather than in one thick layer. Thus, one 7.6-cm-thick layer would carry the same traffic as three 2.5-cm-thick layers.

CONCLUSIONS

1. The strength coefficient of an asphalt overlay is less than the strength coefficient of asphalt concrete for new pavements. It is recommended that, in the design of overlays, the strength coefficient for an asphalt overlay should be taken as half (0.22) the strength coefficient of asphalt concrete for new pavements (0.44).
2. The method for designing an overlay developed in this investigation could be used to determine the thickness of an overlay.

ACKNOWLEDGMENT

The research reported here was conducted under the general supervision of Jack H. Dillard of the Virginia Highway and Transportation Research Council. Frequent discussions with C. S. Hughes and K. H. McGhee were very helpful. The research was done as part of a Federally Coordinated Program project with funds administered by the Federal Highway Administration. The opinions, findings, and conclusions expressed are mine and not necessarily those of the sponsoring agencies.

REFERENCE

1. The AASHO Road Test: Report 5—Pavement Research. HRB, Special Rept. 61E, 1962.

Publication of this paper sponsored by Committee on Pavement Rehabilitation Design.

Analytical Study of Minimization of Reflection Cracking in Asphalt Concrete Overlays by Use of a Rubber-Asphalt Interlayer

N. F. Coetzee and C. L. Monismith, Department of Civil Engineering and Institute of Transportation Studies, University of California, Berkeley

The problem of the reflection cracking that is associated with the rehabilitation of existing cracked pavements by the application of an overlay is considered. A general-purpose finite-element program was used to determine the stresses in the overlay at the discontinuities in the underlying pavement, focusing on the effect of a rubber-asphalt stress-absorbing-membrane interlayer on these stresses. A number of variables—the thickness and stiffness of the overlay, interlayer, cracked layer, and subgrade as well as the crack width—were investigated for a specific load condition.

It is shown that, under certain conditions, the inclusion of an interlayer membrane will significantly reduce the crack-induced stresses in the overlay and, hence, by inference, the probability of reflection cracking. Most of the analyses were directed at traffic-load-associated stresses, but a single thermal-stress analysis indicated that an interlayer is effective in reducing these stresses also.

Asphalt concrete (AC) overlays are widely used for the rehabilitation of AC and portland cement concrete (PCC) pavements in need of additional load-carrying capacity. There are many empirically and theoretically based methods for the design of such overlays; in general, these methods give thickness requirements adequate to provide the structural strength needed to accommodate anticipated traffic volumes and loadings for a projected design life. However, although these overlays are structurally functional, they are susceptible to the development of cracks caused by the reflection of cracking patterns in the underlying pavement.

The mechanisms for the development of these reflection cracks in overlays are not fully understood but are believed to be related to the transfer of high stresses to the underside of the overlay at discontinuities in the underlying pavement. An approach to relieving these stresses that appears promising is the placement of a thin [6.25 to 9.5-mm (¼ to ⅜-in)] asphalt-rubber membrane of low stiffness and high deformability—a so-called stress-absorbing-membrane interlayer at or near the interface between the underlying pavement and the overlay. Recently reported studies of the field performance of overlaid pavements in Arizona (1, 2) that contain one type of rubber-asphalt-membrane interlayer appear to indicate the merit of such an approach and have led to the proposal of testing methods for this material (3).

The analytical study reported in this paper was undertaken to provide some insight as to the efficacy of such an approach and some guidelines for the use of these interlayers.

In this study, responses were investigated of overlaid pavements with and without rubber-asphalt-membrane interlayers to surface loads representative of heavy truck traffic and to temperature changes at the pavement surface. The pavement system was represented by a finite-element idealization, and the distribution of stress in the overlay system in the vicinity of a crack in the existing pavement was examined.

The effects were determined of a number of variables on the stresses resulting from a specific load applied to the surface of the overlay directly above the crack. The variables used include the following:

1. Thickness and stiffness of the rubber-asphalt layer,
2. Thickness and stiffness of the AC overlay,
3. Stiffness of the existing cracked surfacing, and
4. Crack width in the existing surface.

Luther, Majidzadeh, and Chang (4) have also examined the stresses in the vicinity of a crack by using a prismatic-solid finite-element program and a fracture-mechanics approach.

In addition, the stresses in the vicinity of the crack were investigated for a temperature reduction of 22°C (40°F) at the surface of the overlay. This problem has also been examined by Chang, Lytton, and Carpenter (5), who used a fracture-mechanics approach in a study of pavements in west Texas.

The rubber-asphalt membrane characterized for use in this study was a 78:02:20 mixture by weight of paving-grade asphalt, rubber-extender oil, and ground rubber blended together in a conventional distributor truck at a temperature of 175-200°C (350-450°F) and spray applied to the surface. The ingredient imparting the membrane properties is the 20 percent ground rubber fraction, which is a dry, free-flowing blend of 40 percent powdered reclaimed (i.e., devulcanized) rubber and 60 percent ground vulcanized scrap of high natural rubber content.

PAVEMENT SYSTEM

A schematic representation of the pavement system examined in this study is shown in Figure 1. The pavement consists of an AC overlay with or without a rubber-asphalt layer and an existing pavement consisting of a PCC layer, a 300-mm (12-in) thick base course, and a subgrade assumed to have an infinite stiffness at finite depth.

The stiffness characteristics were measured for the rubber-asphalt material and assumed for the other materials. The ranges in stiffness values and layer thicknesses and the crack widths for the PCC layers are summarized below (1 MPa = 145 lbf/in^2 and 1 mm = 0.04 in).

Item	Symbol	Value
AC		
Stiffness (MPa)	E_{ac}	690-10 300
Thickness (mm)	t_{ac}	50-100
Rubber-asphalt interlayer		
Stiffness (MPa)	E_{ra}	6.9-138
Thickness (mm)	t_{ra}	3.2-12.5
PCC		
Stiffness (MPa)	E_{pcc}	6900-27 600
Thickness (mm)	t_{pcc}	100 and 200
Crack width (mm)		6.25 and 12.5
Base course		
Stiffness (MPa)		138
Thickness (mm)		300
Subgrade		
Stiffness (MPa)		34.5 and 69.0
Thickness (mm)		300 and 450

STIFFNESS CHARACTERISTICS OF RUBBER-ASPHALT MATERIAL

Stiffness characteristics of the rubber-asphalt material were determined at two modes of loading—creep and constant rate of strain.

The creep tests were performed in July 1977 on a retained sample of the rubber-asphalt membrane placed on McDowell Road, west of Phoenix, in Maricopa County, Arizona, and obtained in March 1977. These tests gave stiffnesses of 52-25 MPa (7500-3600 lbf/in^2) for loading times representative of moving traffic (0.02-0.05 s) at 21°C (70°F). Based on these data, a value of 34.5 MPa (5000 lbf/in^2) was selected and used for the majority of the analyses. More recently (December 1977), the constant-rate-of-strain tests at 24°C (75°F) gave values of rubber-asphalt stiffness of 9.0-4.5 MPa (1300-650 lbf/in^2) for the same loading time, based on the data plotted in Figure 2. Although a satisfactory explanation for the differences is not available at present, a few additional analyses were performed using stiffnesses for the rubber-asphalt layer as low as 6.9 MPa (1000 lbf/in^2).

FINITE-ELEMENT ANALYSES

The pavement structure was analyzed for traffic loads by using the finite-element program ANSR-1. The two-dimensional finite-element idealization of the pavement structure of Figure 1 is shown in Figure 3. All materials are assumed to be linear elastic and isotropic; a planar strain condition is also assumed (for this assumption, the pavement and load extend to infinity in a direction normal to the plane of the diagram). The actual mesh used to analyze the structure is not shown because

some very small elements [as small as 1.6×0.4-mm (1/16 by 1/64-in) were required at the crack tip in the overlay where very high stress gradients were expected.

Table 1 summarizes the various conditions that were analyzed; there were 48 computer determinations. A total of 106 finite elements were used for cases 1-4, and 115 elements were used for case 5. Approximately 15 additional computer runs were made to validate the results obtained by using the ANSR-1 program. In these comparisons both a layered-elastic-system program (ELSYM5) and the 2D-SAP program were used. Considering the various assumptions required, these comparisons provided sufficient evidence that the ANSR program was giving a reasonable representation of the situation analyzed.

The output of the finite-element program allows plotting the stress or strain distributions throughout the

Figure 1. Schematic representation of pavement structure.

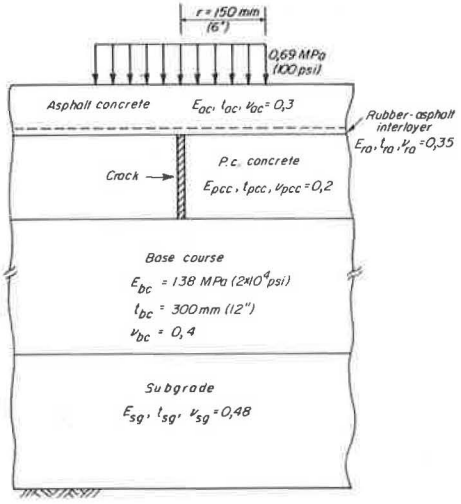

Figure 2. Determinations of creep compliance of rubber asphalt: constant strain rate tests at 21°C.

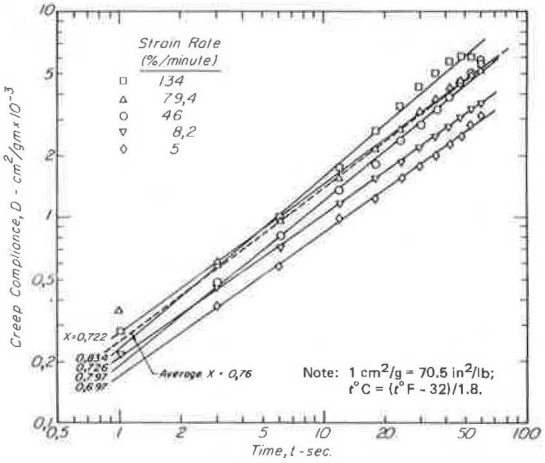

Figure 3. Schematic finite-element representation of pavement structure.

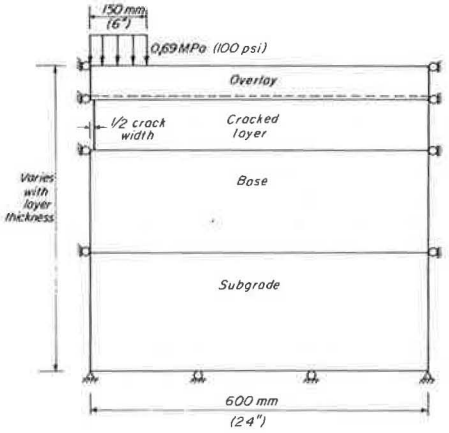

Table 1. Analysis conditions.

Case	Modulus (MPa) AC	Rubber Asphalt	PCC	Subgrade	Thickness (mm) AC	Rubber Asphalt	PCC	Subgrade	Crack Width (mm)
1	690	34.5	13 800	69.0	50	6.25	200	300	12.5
	690	34.5	13 800	69.0	50	6.25	100	300	12.5
	690	34.5	13 800	69.0	75	6.25	200	300	12.5
	690	34.5	13 800	69.0	100	6.25	200	300	12.5
	2 070	34.5	13 800	69.0	50	6.25	200	300	12.5
	3 450	34.5	13 800	69.0	50	6.25	200	300	12.5
	5 175	34.5	13 800	69.0	50	6.25	200	300	12.5
	6 900	34.5	13 800	69.0	50	6.25	200	300	12.5
	10 350	34.5	13 800	69.0	50	6.25	200	300	12.5
	6 900	34.5	6 900	69.0	50	6.25	200	300	12.5
	6 900	34.5	20 700	69.0	50	6.25	200	300	12.5
	6 900	34.5	27 600	69.0	50	6.25	200	300	12.5
	690	6.9	13 800	69.0	50	6.25	200	300	12.5
	690	20.7	13 800	69.0	50	6.25	200	300	12.5
	690	69.0	13 800	69.0	50	6.25	200	300	12.5
	690	103.5	13 800	69.0	50	6.25	200	300	12.5
	690	138.0	13 800	69.0	50	6.25	200	300	12.5
	690	34.5	13 800	69.0	50	6.25	200	300	6.25
2	690	34.5	13 800	34.5	50	6.25	200	300	12.5
	690	34.5	13 800	34.5	50	6.25	100	300	12.5
3	690	34.5	13 800	34.5	50	6.25	200	450	12.5
	690	34.5	13 800	34.5	50	6.25	100	450	12.5
4	690	34.5	13 800	69.0	50	6.25	200	450	12.5
	690	34.5	13 800	69.0	50	6.25	100	450	12.5
5	690	34.5	13 800	69.0	50	3.13	200	300	12.5
	690	34.5	13 800	69.0	50	3.13	100	300	12.5
	690	34.5	13 800	69.0	50	9.5	200	300	12.5
	690	34.5	13 800	69.0	50	12.5	200	300	12.5

Note: 1 MPa = 145 lbf/in²; 1 mm = 0.04 in.

Figure 4. Effective stress distribution: case 1—a 200-mm portland cement concrete pavement (a) with a rubber-asphalt interlayer and (b) without a rubber-asphalt interlayer.

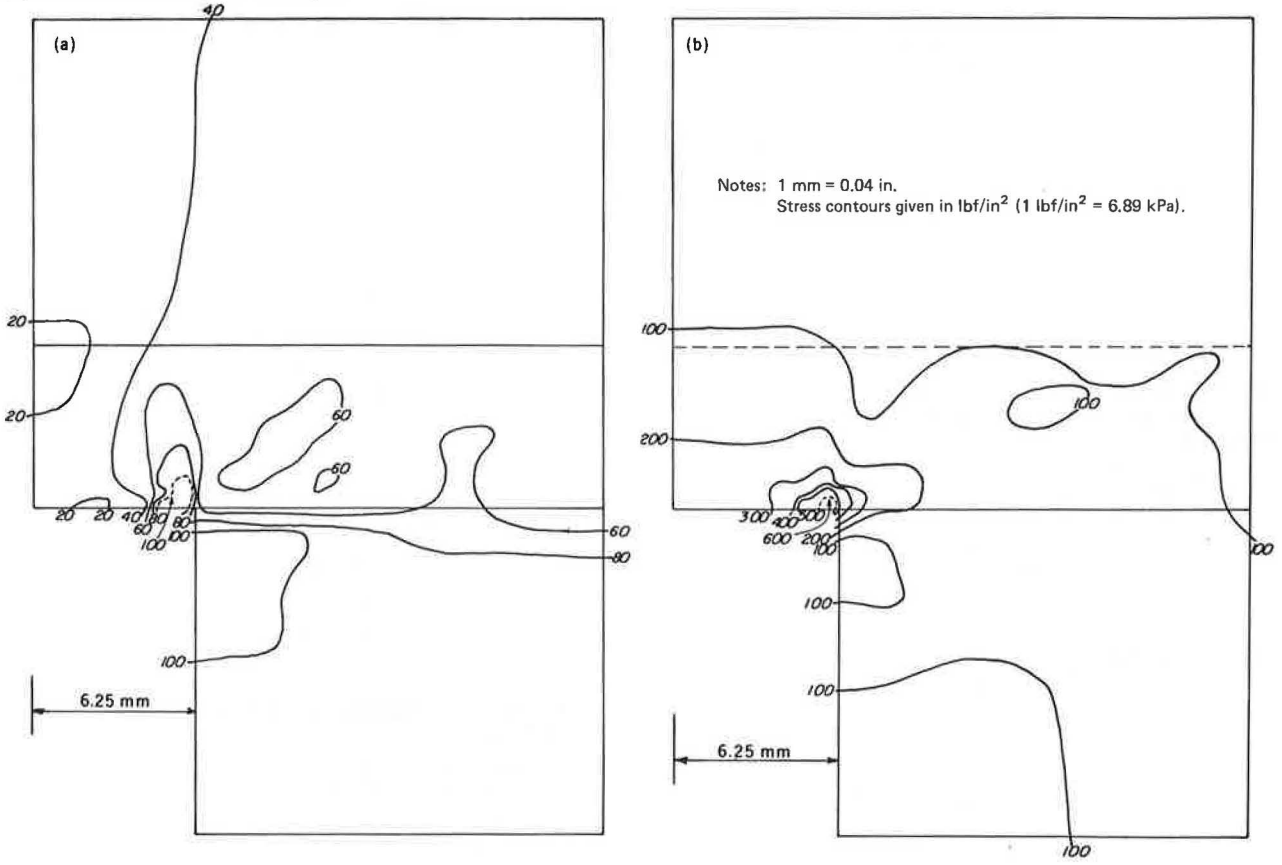

Figure 5. Shear strain distribution: case 1—a 200-mm portland cement concrete pavement (a) with a rubber-asphalt interlayer and (b) without a rubber-asphalt interlayer.

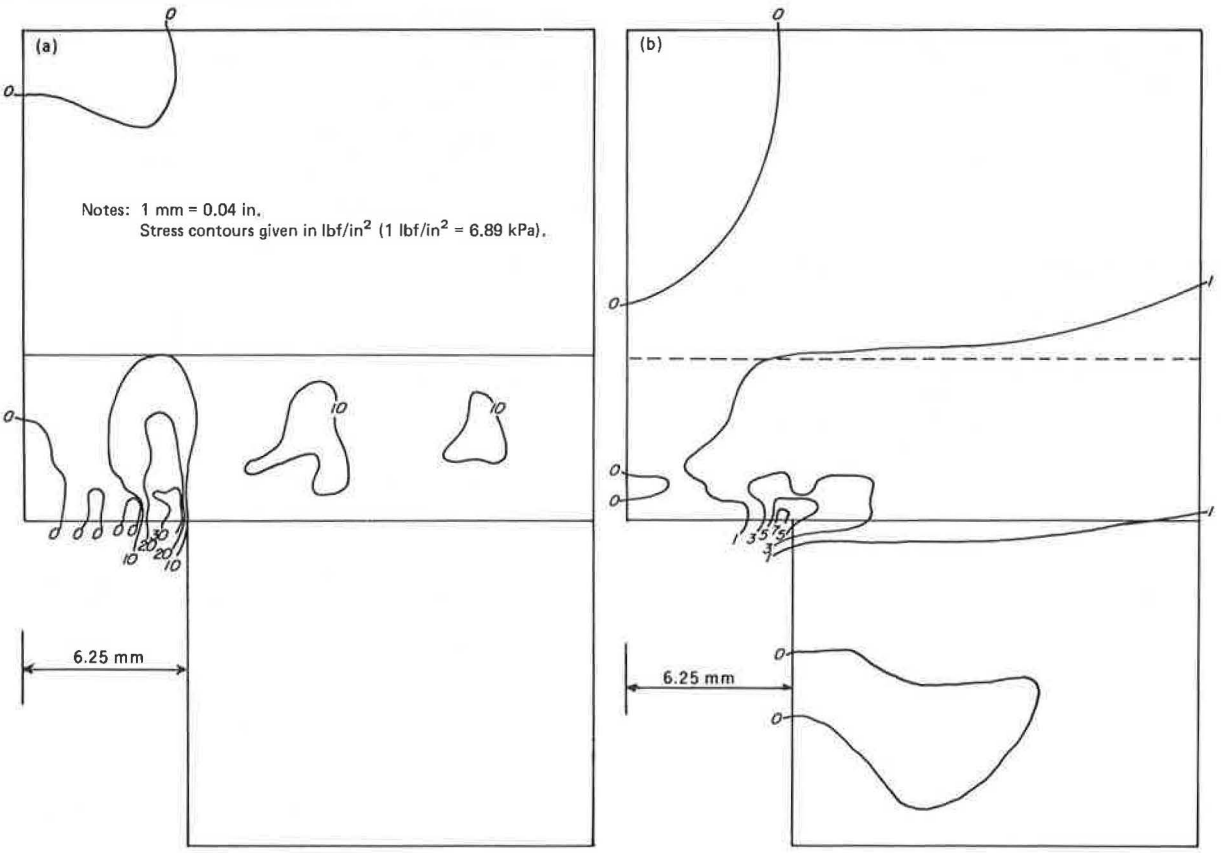

Figure 6. Position (x) at which crack-tip stress is determined.

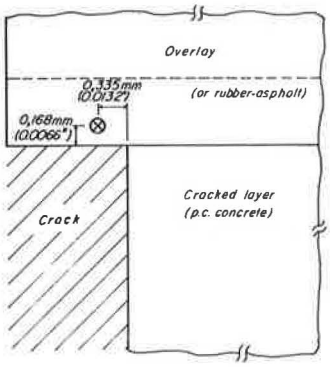

Figure 7. Effect of subgrade stiffness and thickness and thickness of portland cement concrete on effective stress at crack tip.

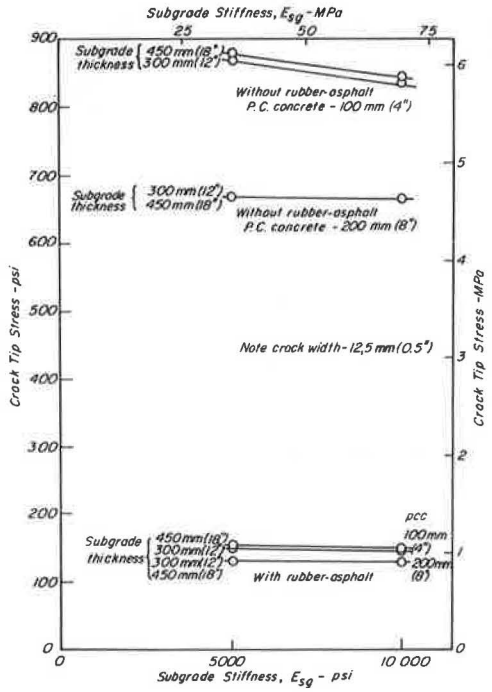

analyzed section. Figures 4 and 5, which represent the small section at the crack tip, are typical of these and illustrate the stress-concentrating effect of the discontinuity. (The finite-element program ANSR was designed for U.S. customary units only; therefore, values in Figures 4, 5, and 16 are not given in SI units.) Figure 5 also begins to provide insight into the so-called stress-absorbing mechanism; viz., that the low-modulus material apparently stores strain energy at low stress and high strain levels, but does not transfer the high strains to the AC overlay or rupture. Because of the difficulty of comparing plots of stress distributions, the results of the analysis presented below, i.e., the effective stresses defined according to the von Mises criterion as

$$(1/\sqrt{2})[(\sigma_1 - \sigma_3)^2 + (\sigma_2 - \sigma_3)^2 + (\sigma_3 - \sigma_1)^2]^{1/2} \quad (1)$$

are for a specific location (see Figure 6) in the overlay or the rubber asphalt, when it is present, adjacent to the crack. This is the point closest to the crack tip for which output is available from the ANSR program. These stresses were selected because they were considered to

Figure 8. Effect of overlay thickness on effective stress at crack tip.

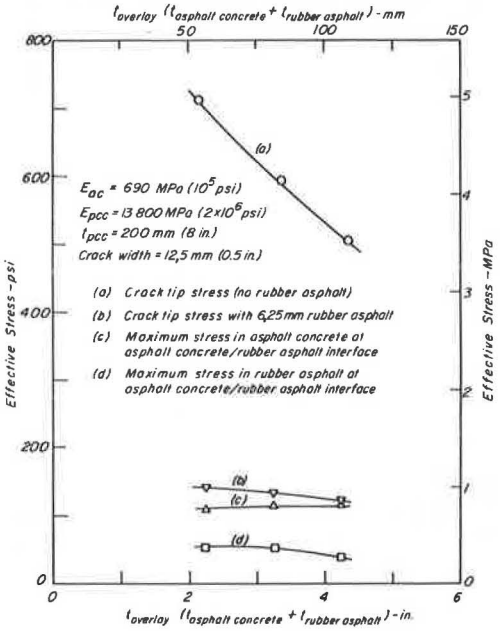

Figure 9. Effect of interlayer thickness on the effective stress at crack tip.

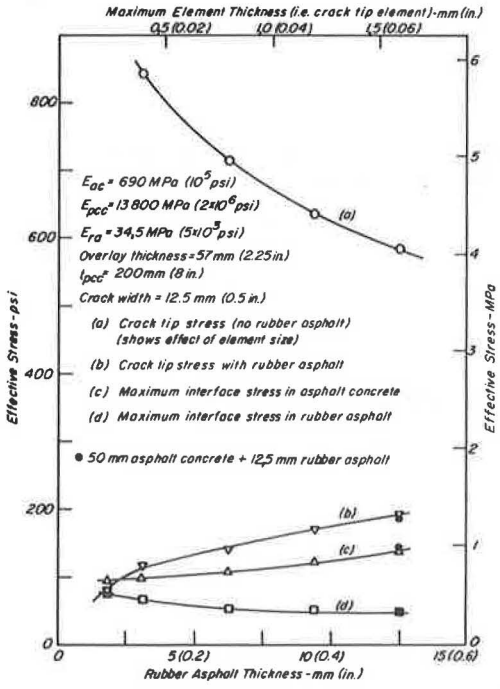

be a realistic determinant for fracture (cracking) under the triaxial stress state existing in the overlay pavement.

COMPUTATIONAL RESULTS

Figures 7-14 illustrate the effects of the various conditions described in Table 1 on the effective stress at the crack tip.

Figure 7 shows that the effect of the rubber-asphalt layer is significant; the stresses in the pavement that contains this layer are one-sixth to one-eighth those in

Figure 10. Effect of rubber-asphalt stiffness on crack-tip stress.

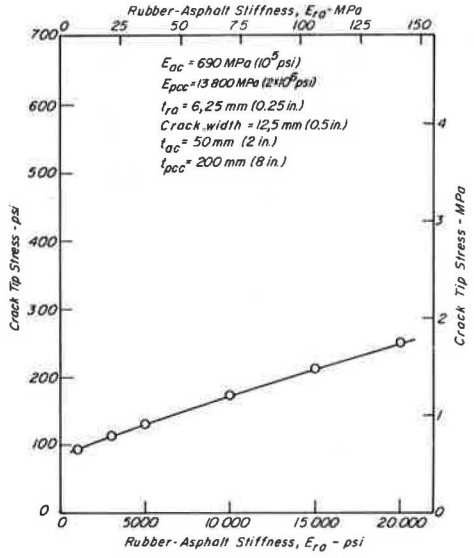

Figure 11. Effect of stiffness of asphalt concrete on crack-tip stress.

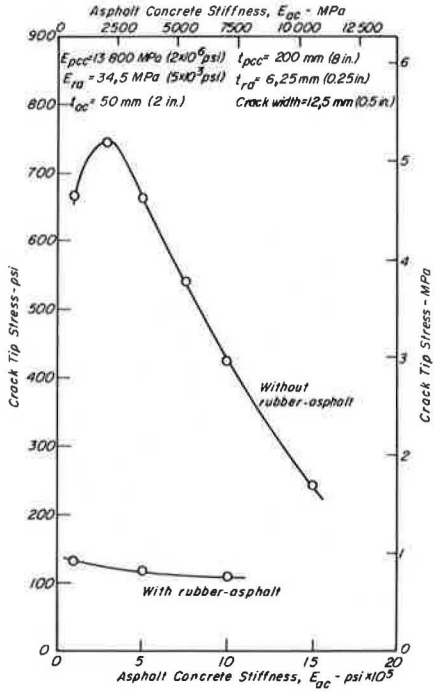

Figure 12. Effect of stiffness of portland cement concrete on crack-tip stress.

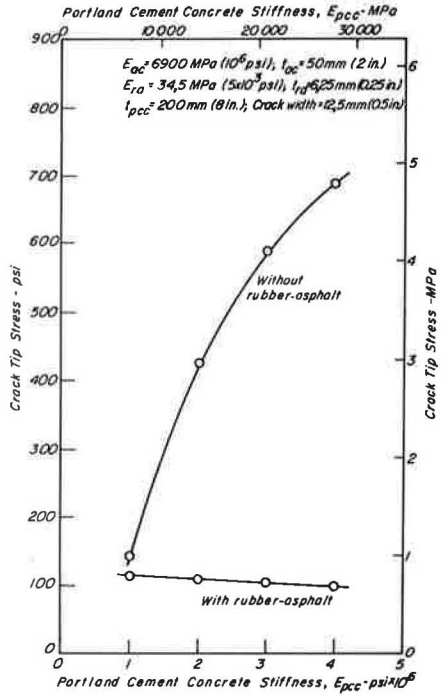

Figure 13. Effect of ratio stiffness of asphalt concrete to stiffness of portland cement concrete on crack-tip stress.

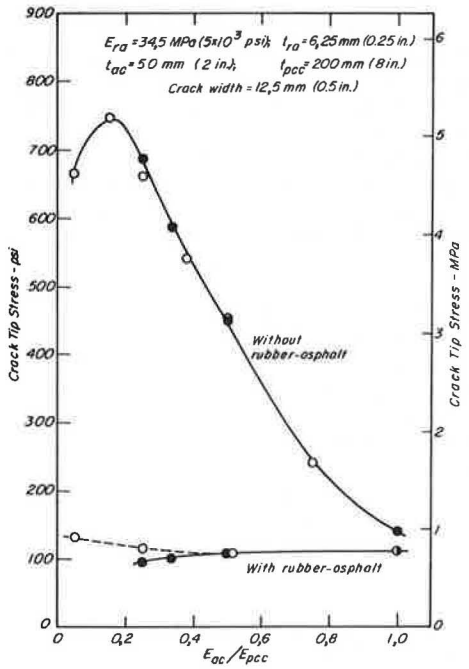

the pavement that does not contain such a layer. The thickness of the PCC layer has only a small effect on the stresses, and the effects of subgrade stiffness and thickness are minimal.

Figure 8 illustrates that the thickness of the AC overlay ($t_{overlay}$) has a significant effect on the stress at the crack tip in the pavement that does not have a rubber-asphalt layer, but little effect on that which does. [In Figure 8, interlayer thickness is constant at 6.4 mm (0.25 in).] An analysis of this type could be most helpful in assessing the trade-off between the thickness of the AC layer and the inclusion of the rubber-asphalt layer. For example, as a rough approximation for the particular situation represented by Figure 8, there appears to be a stress relief of about 0.7 MPa (100 lbf/in^2) at the crack tip for each additional 25 mm (1 in) in thickness of AC. Because there is an approximately 3.8-MPa (550-lbf/in^2) difference in stress levels between curves (a) and (b) at $t_{overlay}$ = 57 mm (2.25 in), it would seem that the pavement that does not have an interlayer would require an additional 140 mm (5.5 in) of AC [i.e., $t_{overlay}$ = 57 mm + 140 mm = 197 mm (7.75 in)] to achieve the same crack-tip stress level as 50 mm (2 in) of AC and a 6.4-mm rubber-

Figure 14. Effect of crack width on crack-tip stress.

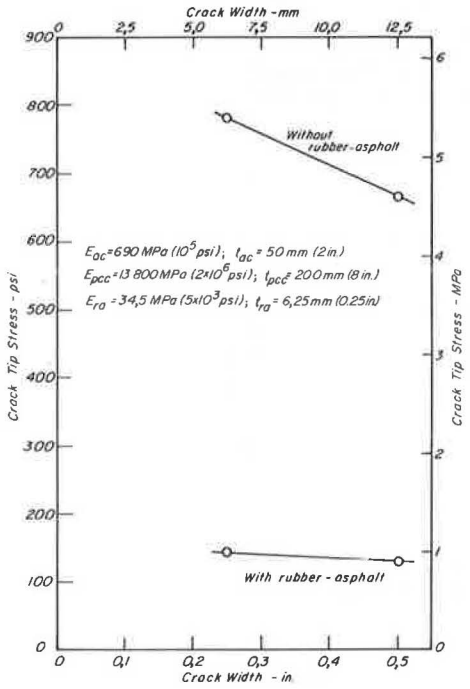

Table 2. Material properties used in thermal-stress determination.

Layer	Modulus (MPa)	Poisson's Ratio	Coefficient of Linear Expansion per °C	Thickness (mm)
Asphalt concrete	690	0.3	22.5×10^{-6}	50
Rubber asphalt	13.8	0.35	27.0×10^{-6}	6.25
Portland cement concrete	13 800	0.2	7.0×10^{-6}	200
Aggregate base	138	0.4	18.0×10^{-6}	300
Subgrade	69	0.48	18.0×10^{-6}	300

Note: 1 MPa = 145 lbf/in²; t°C = (t°F - 32)/1.8; 1 mm = 0.04 in.

Figure 15. Temperature profile for 22.2°C decrease in temperature at pavement surface.

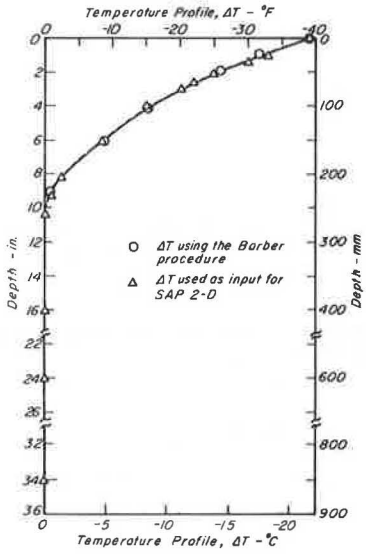

asphalt interlayer. It is interesting that, for this thickness of rubber asphalt, at least, the maximum stress in the AC at its interface with the rubber asphalt is about the same independent of overlay thickness.

Curve (a) of Figure 9 illustrates the effect of element size on crack-tip stress for an overlay thickness of 57 mm on a pavement that does not have a rubber-asphalt layer. The elements varied in size from 1.6×0.24 mm (0.0625×0.009 375 in) (an aspect ratio of 6.7:1) to 1.6×1.6 mm, (an aspect ratio of 1:1). Generally, an aspect ratio of 2:1 or less is recommended because the increased accuracy expected from the smaller elements in the thinner layers will offset the effect of the less desirable aspect ratio.

Curve (b) of Figure 9 shows that the crack-tip stress decreases as the interlayer thickness decreases. This is expected in this case because the total overlay thickness was maintained constant; a decrease in interlayer thickness is equal to a corresponding increase in AC thickness. (The effect of element size, as noted above, must be considered here as well.)

As the interlayer thickness decreases, it would appear reasonable that the stresses at the interface of the AC and the rubber asphalt should approach the stresses of curves (a) and (b); i.e., the interface stress of curve (d) (in rubber asphalt) should converge with the crack-tip stress (curve b), which in fact it appears to do.

Similarly, it would be expected that the maximum interface stress in the AC (curve c) would first decrease with decreasing interlayer thickness (increasing AC thickness) and then to increase rapidly as the AC layer approaches the high strain zone at the crack tip; i.e., curves (a) and (c) should converge. From an examination of Figure 9, it would appear that this may occur. At an interlayer thickness of 2.25 mm (0.09 in), the AC interface stress is larger than the crack-tip stress in the rubber asphalt.

Figure 9 also shows the results of an analysis that compared stresses for 50 mm (2 in) of AC plus 12.5 mm (0.5 in) of rubber asphalt with those for 44.5 mm (1.75 in) AC plus 12.5 mm (0.5 in) of rubber asphalt. The results are essentially the same.

Figure 10 shows that, as the modulus of the rubber asphalt decreases, the crack-tip stress also decreases; this leads, in turn, to the conclusion that the estimated stresses at the crack tip in the pavements that contain rubber asphalt given thus far are probably larger than those that actually occur. As pointed out in the analysis of the creep-test data, a rubber-asphalt-modulus value of 34.5 MPa is probably too high; a value of 10.3-13.8 MPa (1500-2000 lbf/in²) may (possibly) be more acceptable. If this is the case, then from Figure 9, it can be expected that the effect of the lower modulus would be even more significant than already shown.

Figure 11 illustrates the effect of AC stiffness on crack-tip stress for a constant cracked-layer modulus of 13 800 MPa (2 000 000 lbf/in²). Figure 12 illustrates the effect of the modulus of the cracked layer at an AC modulus of 6900 MPa (1 000 000 lbf/in²). Figure 13 combines the data from Figures 11 and 12 and normalizes them by considering the ratio of the modulus of the AC layer to that of the cracked layer. The resulting curve is similar to that shown in Figure 11, and the points in Figure 13 appear to fit this curve well, indicating that this ratio is very important in determining crack-tip stress level, more so than the actual modulus of either layer. It will be noted that, the closer the modulus ratio is to unity, the better the performance of the overlay that does not have a rubber-asphalt interlayer as compared with the overlay that does.

Figure 14 illustrates the effect of variation of crack width. This is the most difficult task to perform on the finite-element mesh. However, the increase in stress found as the crack width decreased is consistent with what a theoretical (fracture mechanics) approach would predict.

Figure 16. Horizontal stresses resulting from 22.2°C decrease in temperature at overlay pavement surface: a 200-mm portland cement concrete pavement (a) with a rubber-asphalt interlayer and (b) without a rubber-asphalt interlayer.

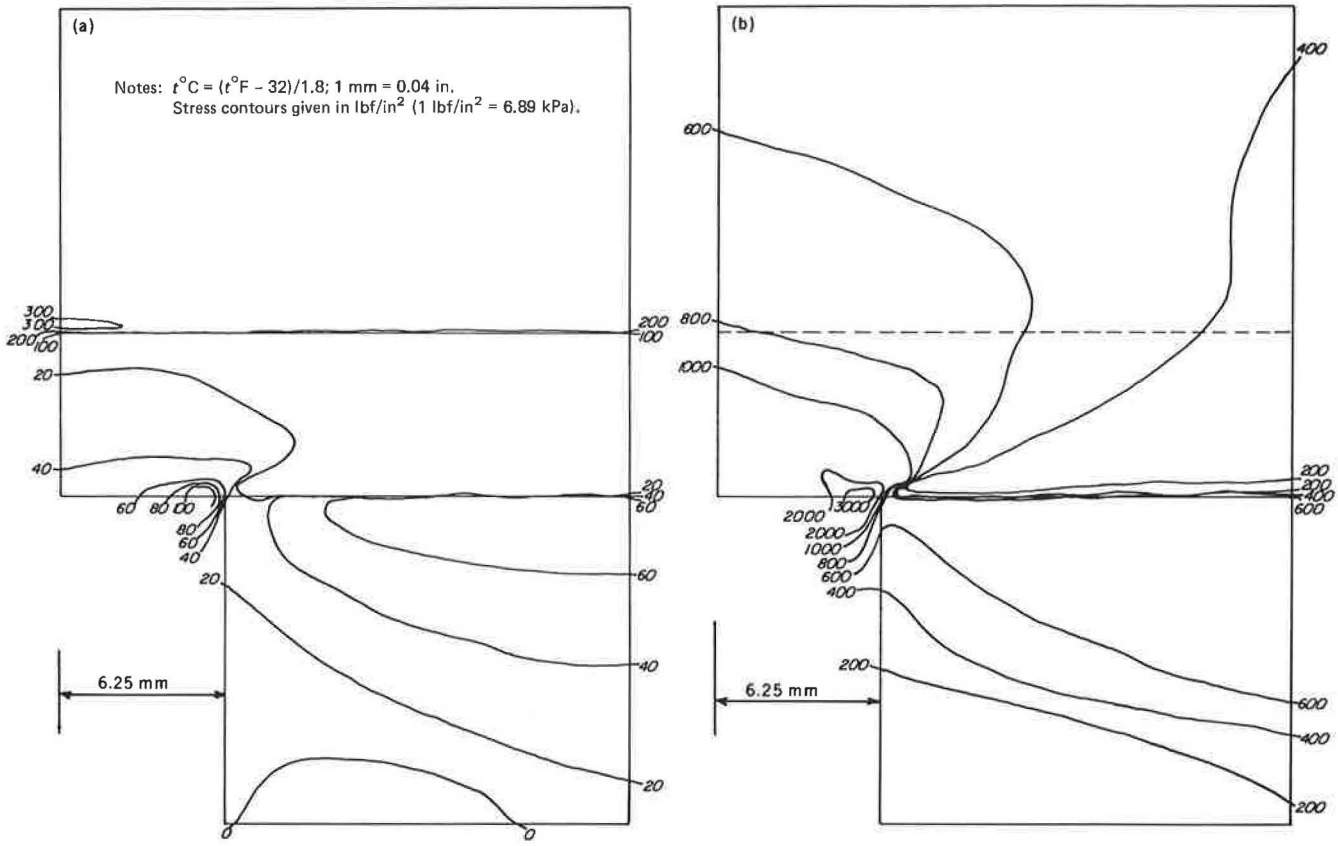

A limited analysis was conducted by using the SAP program to estimate the stresses that result from temperature changes. The materials properties of the system examined are given in Table 2, and its temperature profile is shown in Figure 15. The stress distributions in the vicinity of the crack are illustrated in Figure 16 for a temperature decrease of 22°C at the pavement surface at a constant AC modulus. However, as shown in Figure 15, this temperature change is attenuated with depth and, in reality, the modulus of AC is a time-dependent parameter. Thus, it is probable that the differences in stress between the two cases are not as large as indicated in Figure 16, although the effect of the interlayer in reducing thermally induced stresses in the overlay is obviously significant.

SUMMARY

Consideration of Figures 4, 5, and 16 shows that the reflection-cracking problem can, in the first stage at least, be directly attributed to the high stresses that will develop in the overlay as a result of the discontinuities in the cracked layer. It is suggested that the problem of load-associated reflection cracking should be considered in two stages: viz., first, attention should be directed to the attenuation of the high stress that occurs as a result of the cracks and, second, because the maximum vertical deflections of the overlay occur at these cracks, a fatigue analysis should be carried out for the overlay at these points after the stress-concentrating effect of the cracks has been nullified.

For thermal stresses, of course, only the first stage is of interest. As is apparent from Figures 7-14 and 16, a low-modulus interlayer (rubber asphalt) can significantly inhibit both load- and temperature-change-induced reflection cracking, particularly when the modulus of the proposed overlay is of the order of 0.1-0.25 that of the cracked-layer modulus. This investigation has also shown that crack width, interlayer modulus, and overlay thickness appear to have significant effects on crack-tip stress, but that the ratio of the modulus of the overlay to that of the cracked layer appears to be the major factor involved.

It should be noted that this study has focused on crack-tip stress. When a rubber-asphalt interlayer is used, this crack-tip stress occurs in the interlayer; if the strength of the interlayer material is such that the crack-tip stress does not cause it to yield, then the crack-tip stresses for the cases that do not have interlayers should be compared with the maximum stress in the AC layer for the case that has an interlayer. In general, this stress is lower than the crack-tip stress, as can be seen by comparing curves (b) and (c) in Figures 8 and 9. Furthermore, because the rubber-asphalt modulus used for these analyses is probably too high, the crack-tip stresses when the interlayer is included are conservative (high).

The finite-element representation used results in high stresses at the lower tip of the crack, i.e., in the granular base course. To simulate the yielding, further analyses were made in which the restraints on this material were released to such an extent that the stress in the base course was at an acceptable level. The effect of this was to marginally increase the crack-tip stresses, so that the values plotted can be taken to be valid.

Finally, it should be pointed out that the analyses typified the interlayer as a low-modulus material exhibiting linear elastic behavior. Stress and strain distributions (e.g., Figures 4 and 5) indicate also that the material should be able to withstand high strain levels

without rupturing. From the limited tests performed on the rubber asphalt, it appears to have all the desirable properties, an observation that is supported by reports (1, 2) of its successful performance in practice.

REFERENCES

1. G. R. Morris and G. H. McDonald. Asphalt-Rubber Stress-Absorbing Membranes: Field Performance and State of the Art. TRB, Transportation Research Record 595, 1976, pp. 52-58.
2. W. O. Ford and H. G. Lansdon. Development and Construction of Asphalt-Rubber Stress-Absorbing Membranes. Paper presented at 55th Annual Conference of the Western Association of State Highway and Transportation Officials, Seattle, June 19, 1976.
3. R. A. Jimenez. Testing Methods for Asphalt-Rubber: Final Report—Phase 1. Arizona Department of Transportation, Phoenix, Rept. ADOT-RS-15(164), Jan. 1978.
4. M. S. Luther, K. Majidzadeh, and C. W. Chang. Mechanistic Investigation of Reflection Cracking of Asphalt Overlays. TRB, Transportation Research Record 572, 1976, pp. 111-122.
5. H. S. Chang, R. L. Lytton, and S. H. Carpenter. Prediction of Thermal Reflection Cracking in West Texas. Texas Transportation Institute, Texas A&M Univ., College Station, Rept. TTI-2-73-18-3, March 1976.

Publication of this paper sponsored by Committee on Pavement Rehabilitation Design.

Attempts to Reduce Reflection Cracking of Bituminous Concrete Overlays on Portland Cement Concrete Pavements

K. H. McGhee, Virginia Highway and Transportation Research Council, Charlottesville

Studies of methods used in Virginia to reduce the incidence of reflection cracking when portland cement concrete pavements or bases are overlaid with asphalt concrete are reported. The methods discussed are (a) the use of sand to break the bond between the portland cement concrete pavement and the asphalt overlay and (b) the use of a fabric that has a high tensile strength as a stress-relieving layer between the asphalt layer and the concrete base. The studies showed that neither the sand bond breaker nor the high-strength fabrics are effective in reducing reflection cracking where differential vertical joint movements are a significant factor. Further studies showed that high-strength fabrics can delay the onset of reflection cracking but that such cracking will eventually develop under the application of repetitive wheel loadings.

The transverse joints in rigid pavements commonly reflect through bituminous concrete overlays in a short time. Many highway engineers believe that these reflection cracks are detrimental to pavement riding quality, and others believe that they are generators of future maintenance problems because they provide surface water ready access to subsurface pavement layers (1). Recent studies support this latter belief; it has been reported that a crack only 0.9 mm (0.035 in) wide will admit 70 percent of the surface water that falls on a pavement sloped 1.25 percent under a 50-mm/h (2-in/h) rate of precipitation (2).

METHODS USED

Numerous attempts to reduce reflection cracking have been reported in the literature. A good summary of those that have been at least partially successful is given in the National Cooperative Highway Research Program Synthesis on Pavement Rehabilitation (1). In that document, most of the methods attempted are grouped into four general classifications: (a) increased thickness of the asphalt concrete (AC) overlay, (b) special treatment of the existing PCC pavement, (c) special consideration of the AC overlay design, and (d) treatment of joints and cracks.

In Virginia, most of the methods in categories a through c have been rejected for economic or other reasons. The category d methods used in Virginia all consist of some method of breaking the bond or otherwise relieving the stress between the PCC and the bituminous concrete overlay. The first attempts to provide a bond breaker were reported by Hughes, who found that a thin layer of sand spread on either side of the PCC pavement joints before the application of a bituminous concrete overlay was partially successful in reducing reflection cracking. In his studies, an asphalt-emulsion tack coat was applied at a rate of 0.23-0.46 L/m^2 (0.05-0.10 gal/yd^2) for a distance of 225-300 mm (9-12 in) on either side of the transverse joints, and the class A sand sieved to pass a 9.5-mm (3/8-in) sieve was applied over the tack coat to a thickness of approximately 6 mm (1/4 in). A 59 to 95-kg/m^2 (100 to 175-lb/yd^2) AC overlay (85-100 penetration grade asphalt) was applied over the pavement surface and the sanded joints. Joint spacings were 9 m (30 ft). However, of the three projects treated in such a manner, only one showed any indication of fewer reflection cracks on the joints treated with sand. There was no apparent reason for any differences in performance among the three projects, and nine years later, some of the joints still had not reflected through the best-performing project, that located on US-13.

The next significant attempt to reduce reflection cracking, also reported by Hughes, involved the use of a nonwoven polypropylene fabric spanning the reflective cracks on a previously overlaid concrete pavement on US-460 (2). The polypropylene had a high tensile strength and was reported to prevent horizontal overstressing of the overlay. Supposedly, at points of stress concentration such as transverse joints or cracks, the material would prevent reflection cracking. Again, the